

## FLUXES OF PARTICLES IN SECONDARY BEAMS

L. Koester

September 18, 1967

Estimates of secondary beam fluxes from 200 GeV or 300 GeV protons have been made by numerous authors.<sup>1</sup> What, then, are the purposes of this report? Some of the principal aims are the following.

1. To review the literature to evaluate the discrepancies in estimates by different authors and to reach a satisfactory decision as to how to make our own estimates. In this connection, we may point out sources of experimental data expected to be forthcoming in the near future.

2. To make some specific graphs of numbers of particles expected in the beams under consideration for the 200 GeV accelerator. At least two kinds of design options are influenced by these graphs, especially if they are extended to other primary energies.

- a. The geometry of the secondary beams may be arranged to accept particles either in a cone centered on the primary beam direction or in slit apertures at small angles to this direction.
- b. The capability to vary the machine energy with reciprocal increase in proton intensity per minute (for example, the ring filling time required by the booster accelerator) affects the cost. Is it worth it in terms of improved experimental conditions?

3. To relate the production of neutrino beams with that of the usual secondary beams and to see if similar considerations of energy and intensity are valid.

#### I. Review of Secondary Flux Estimates

Looking at the reports<sup>1</sup> of 200-300 GeV study groups since 1961, one finds that 2 or 3 different procedures have been used to estimate secondary particle fluxes. Cocconi, Koester, and Perkins<sup>1</sup> (CKP) developed a particularly simple formula based on evidence from cosmic rays and 30 BeV aacc accelerators that (a) the average transverse momentum distribution is the same for all secondaries and is independent of their longitudinal momentum. It seems to be well represented by a Boltzmann-like expression with 0.35 GeV/c as the average transverse momentum. (b) The shape of the longitudinal momentum spectrum seems to remain the same, approximately exponential for large values. (c) The average multiplicity  $n_s$  of secondaries from nucleon-nucleon collisions increases as  $E_0^{1/4}$ , where  $E_0$  is the primary energy, and the fraction of the available energy given to secondaries does not change radically with  $E_0$  between 10 and  $10^4$  GeV. Thus if T is the average energy of the secondaries, the above implies that

$$n_s T \sim E_0;$$

hence 
$$T \sim E_0^{3/4}.$$

Note that T is practically equal to the average longitudinal momentum.

(d) The spectra of secondaries observed from targets of various elements were the same apart from a normalizing factor near unity.

The CKP formula is thus a product of the transverse and longitudinal momentum distributions. Expressed in terms of one interacting proton, unit solid angle, and 1 GeV/c momentum interval, it is

$$\frac{d^2N}{dp \cdot d\Omega} = \frac{n_{\pi} \cdot p^2}{2\pi \cdot p_0^2 \cdot T} \cdot e^{-p/\pi} \cdot e^{-p \cdot \theta/p_0} \quad (1)$$

where  $n_{\pi} = \frac{n_{\pi}}{6} = 0.45 \cdot E_0^{1/4}$  is the number of pions of one charge, (The division by 6 results from the 3 types of pions going forward only in the CMS.)  $T = 0.3 E_0^{3/4}$  is the average total (longitudinal) momentum.  $P_0 = 0.18$  GeV/c is half the average transverse momentum.

Trilling<sup>2</sup> criticized the CKP formula (1) on the grounds that it makes no distinction between  $\pi^+$  and  $\pi^-$  fluxes and that it did not fit the newer, more complete data at several energies below 30 BeV, particularly in regard to dependence on primary energy. To improve the quality of the fitting, he proposed a two-term expression based on a semi-empirical model. The high momentum secondaries are attributed to decaying isobars moving practically with the incident proton. The low energy pions, represented by the first term in (2) below, are treated as boil-off secondaries with an average energy proportional

$$\text{to } E_0^{1/2}. \quad \frac{d^2\sigma}{dp \cdot d\Omega} = A \cdot p^2 \cdot \exp\left[-\frac{4.8 p}{E_0^{1/2}} - 2.6 p \cdot E_0^{1/2} \theta^2\right] + \frac{B \cdot p^2}{E_0} \cdot \exp\left[-10.4 \left(\frac{p}{E_0}\right)^2 - 3.9 p \cdot \theta\right] \text{ mb/sr. GeV/c} \quad (2)$$

where  $A(\pi^+) = A(\pi^-) = 53$   
 $B(\pi^+) = 100$   
 $R(\pi^-) = 33$

Trilling's equation (2) results in a double-peaked spectrum shown by the dotted curves in Fig. 1 for 200 GeV incident protons. These curves were taken from reference 2 and are compared with the CKP curves obtained from Eq. (1). Trilling's spectra contain more pions at large momenta and large angles, and fewer around 20-40 GeV/c.

In a rebuttal, Cocconi<sup>3</sup> questioned Trilling's assumptions about the behavior of isobar production as a function of energy and the contribution of the lighter isobars to the production of the most energetic pions. He remarked that Trilling's use of a Gaussian distribution for the transverse momentum (in the first term of (2)), with standard deviation dependent on the momenta of the incident proton as well as the secondary pion, seemed to ignore the most convincing and recurring evidence from cosmic rays and other sources on the constancy of the transverse momentum distribution. Cocconi noted that Hagedorn<sup>4</sup> suggested a reasonable modification to incorporate a secondary particle mass dependence into the transverse momentum distribution. A fitting would have to be done to match the observed values of  $\approx 0.350, 0.450$ , and  $0.650$  GeV/c for the average transverse momentum of  $\pi$ 's, K's, and  $\Sigma$ 's respectively.

Hagedorn and Ranft<sup>4</sup> have developed a statistical thermodynamics of strong interactions at high energies. Their model treats each element of the interacting volume as a virtual fireball, with a temperature and velocity, capable of emitting isotropically in its rest frame according to a thermodynamic momentum spectrum. These fireballs have to be superimposed and transformed to the lab system. The authors' development sounds very

reasonable, but it does not provide a simple way for a novice to compute spectra with a slide rule. They do have programs at the CERN CDC 6600 computer to calculate any spectra (see reference 4, p. 106).

For purposes of comparison, the 300 GeV spectra of Hagedorn and Ranft taken from reference 4 are presented on Fig. 2. On Fig. 3, plotted to the same scale, are the CKP spectra obtained from Eq. (1) with a slide rule. According to the ECFA report<sup>4</sup>, CERN has adopted a policy of using Hagedorn's curves for estimating shielding and CKP for secondary beams.

Recently, Krisch<sup>5</sup> has noted that extrapolating from 12.5 GeV to 200 GeV is only a factor of 4 in the CMS. On the basis of his experimental data<sup>6</sup> from p-p collisions at 12.5 GeV/c, he finds a Gaussian distribution of transverse momenta and interprets the results in terms of 2 fireballs. When his CMS momentum spectra are transformed to the lab system, they may be compared with CKP, etc. One point that he makes is of interest, namely that the multiplicity changes from 3 to 12.5 GeV/c to 6 at 200 GeV/c (from cosmic ray evidence). This factor of 2 agrees with the  $E_0^{1/4}$  multiplicity dependence assumed in (1) above.

Other sources of data hopefully forthcoming soon are the cosmic ray experiments of Jones et al.<sup>7</sup> on Mt. Evans and of Alvarez et al. with balloons.

## II. Graphs

Aside from refinements in spectrum shape, and with the reservations that it is invalid below 1 GeV/c and does not vanish at  $E_0$ , the CKP formula (1) seems to be as good a bet for extrapolating to 200 GeV as any other, and it

is very easy to use with a slide rule. As a check on the parameters used for  $n_4$ ,  $p_0$ , and  $T$  in Eq. (1), the pion spectra for 30 GeV protons were plotted in Fig. 4. along with data points of Anderson et al. <sup>8</sup> which were simply copied from one of Hagedorn's graphs<sup>4</sup>. These same parameters were used for all the computations.

The format of Figs. 1-4 is widely used. To obtain from the <sup>graphs</sup> the number of particles in a beam, multiply the ordinate by (a) the solid angle accepted by the beam transport system at the angle  $\theta$ , (b) the number of incident protons times the probability that they interact, (c) the momentum interval accepted in GeV/c. All of the graphs refer to  $\pi^+$  mesons;  $\pi^-$  are assumed to be the same or slightly fewer in number. For  $K^+$ , CKP estimate 10-15% of  $\pi^+$ ; and for  $K^-$ , 5-10% of  $\pi^+$ . The decay length of the K's must not be overlooked on long beams.

One of the <sup>aims</sup> aims of this work was to compare fluxes from different proton energies. Figs. 1, 2, and 5, all drawn to the same scale for 200, 300, and 100 GeV protons, respectively were made for this purpose. A more convenient format is shown in Figs. 6, 7, and 8, for 100, 200, and 300 GeV incident protons. In these, the ordinate contains a factor (0.01 p) of 1% of the momentum for each abscissa, corresponding to  $\pm 0.5\%$  momentum selection. Then the numbers read from the graphs only need be multiplied by a constant (the solid angle times the number of interacting protons).

### III. Secondary Beam Design Considerations

The graphs display the strong angular dependence of the secondary fluxes. One decision to be made is whether to provide beams at  $\theta = 0$  by placing the target in a magnetic field or to eliminate the magnet and obtain beams at 2.5 mr, etc. A strong argument against the magnet is that it makes the several beams from the same target interdependent. A weaker argument is that the  $\theta = 0$  curve is slightly deceptive. For example, a beam accepting  $\pi \times 10^{-6}$  sr solid angle goes out to  $\theta = 1$  mr. Integrating the angular part of (1) by setting  $\sin \theta = \theta$  gives

$$2\pi \int_0^{1 \text{ mr}} \theta \cdot e^{-p \cdot \theta / p_0} \cdot d\theta = 2\pi \cdot \left(\frac{p_0}{p}\right)^2 \left[ 1 - \frac{p}{p_0} \cdot e^{-\frac{10 \cdot p}{p_0} \cdot \left(10^{-3} + \frac{p_0}{p}\right)} \right] \quad (3)$$

For  $p = 50$  GeV/c, the result is a factor of only  $2.6 \times 10^{-6}$  instead of  $\pi \times 10^{-6}$ ; and of course this factor decreases as the subtended angle increases.

A very interesting feature of the graphs is the dependence on primary energy. Comparison of Figs. 6, 7, and 8 shows that for any pion momentum over 20 GeV/c, one obtains more than twice as many pions at the same production angle, per proton, at 200 GeV as at 100 GeV/c. Thus running the accelerator at a reduced energy with a reciprocal increase in intensity would give no better secondary flux. Perkins<sup>9</sup> used the CKP formula (1) to optimize pion beams quantitatively. Assuming the time average machine proton current to be proportional to  $E_0^{-1}$  and differentiating (1) to maximize,

he showed that the CKP formula predicts maximum pion flux at pion energy  $E$  (with  $\theta = 0$ ) for a machine energy

$$E_0 = E_{opt.} = (1.6E)^{4/3} \quad (4)$$

The the pion intensity  $I$  at the same momentum ( $\approx E$ ) is related to the maximum intensity  $I$  by

$$\frac{I}{I_{max}} = e^{-2} \left( \frac{E_{opt.}}{E_0} \right)^{3/2} \exp \left[ -2 \left( \frac{E_{opt.}}{E_0} \right)^{3/4} \right] \quad (5)$$

It turns out that this dependence on  $E_0$  is not very strong. In particular, running the machine at twice the optimum energy only reduces the pion intensity by 20%. Note that the graphs do not contradict this result. The optimum machine energy for 25 GeV pions is 137 GeV, and 300 GeV for 45 GeV pions.

Some simplifications of Eq. (1) are worth writing. Just multiplying the constants gives

$$\frac{d^2N}{dp.d\Omega} = \frac{7.4 \cdot p^2}{E_0^{1/2}} \cdot \exp \left[ -p \left( \frac{1}{T} + \frac{\theta}{p_0} \right) \right] \quad (6)$$

with  $p_0 = .18 \text{ GeV}/c$  and  $T = 2.3 E_0^{3/4}$ .

Another form useful for scaling is

$$\frac{d^2N}{dp.d\Omega} = \frac{n_+ T}{2\pi p_0^2} \cdot \left( \frac{p}{T} \right)^2 \cdot \exp \left[ -\frac{p}{T} \left\{ 1 + \frac{\theta \cdot T}{p_0} \right\} \right] \quad (7)$$

Since  $(n_+ T)$  is proportional to  $E_0$ , (7) implies that

$$\frac{\frac{d^2N_1}{dp.d\Omega} \left( \frac{E}{T}, \theta T \right)}{\frac{d^2N_2}{dp.d\Omega} \left( E/T, \theta T \right)} = \frac{E_{01}}{E_{02}} \quad (8)$$

#### IV. Neutrino Beam Considerations

Two types of neutrino beams have been under discussion lately.

The narrow band system (NBS) carries a focused beam of  $\pi$ 's and K's with small momentum interval ( $\pm 5\%$  or so) down a decay path and removes the charged particles by sweeping magnets at the end. A modest shield (30-100 m of steel) is sufficient to remove the neutrons, gammas, K<sup>0</sup>'s, etc. at the end. The resulting neutrino spectrum is peaked near its upper limit of .42 times the pion momentum (if one ignores the small contribution from K's).

The wide band system (WBS) uses a horn or something to shoot all possible secondaries down the decay path and stops the  $\mu$ 's (and everything else) with a very massive shield. The WBS delivers many more neutrinos and is no disadvantage in terms of energy resolution because the NBS cannot be considered monoenergetic anyway. The detector must identify each event. The trouble is that the massive shield is so expensive that the NBS would probably be used first. At least, this is the opinion of Perkins,<sup>10, 11</sup> who wrote two good discussions on the subject.

As far as the NBS is concerned, its intensity is proportional to the intensity of pions at a given momentum. The discussion above indicated that higher machine energies were more advantageous. The WBS needs a little more thought. The shield, stopping muons by ionization, has a cost proportional to the energy. Thus one may bring down the cost by operating at reduced energy, in which case he would want to regain as much intensity as possible by increasing the number of protons accelerated per minute.

REFERENCES

1. Cocconi, Koester, and Perkins, UCRL 10022, 167 (1961).  
G. Cocconi, Proceedings of Argonne Accelerator Users Group Meeting, December 1961.
2. G. Trilling, UCID-10148, UCRL-16830, 25 (200 BeV Summer Study Vol. I, 1964-65). See also UCRL 16000 (Blue Book) Vol. I, XIII-1 (1965).
3. G. Cocconi, UCRL 16830 Vol. III, 17 (1966).
4. R. Hagedorn and J. Ranft, CERN/ECFA 67/16 Vol. I, 70 (1967).
5. A. D. Krisch, EA-67-43 NAL Report.
6. Ratner, Edwards, Akerlof, Crabb, Day, Krisch, and Lin, "Pion, Kaon, and Antiproton Production in the Center of Mass in High Energy Proton Proton Collisions," preprint 1967 submitted for publication.
7. L. W. Jones, "A Cosmic Ray Program for the Study of Strong Interaction Physics in the Range of 100-1000 GeV," Technical Report No. 30, Physics Report, University of Michigan, Ann Arbor.
8. Anderson, Bleser, Collins, Fujii, Menes, Turkot, Carrigan, Edelstein, Hien, McMahan, and Nadelhoft - Stoney Brook Conference (1966).
9. D. H. Perkins, UCRL-10022, 231 (1961).
10. D. H. Perkins, UCRL-10022, 222 (1961).
11. D. H. Perkins, CERN/ECFA 66/WG2/US-SGI/DHP-1/Rev., (1967).

# 200 GEV PRIMARY PROTON ENERGY

CKP PIONS OF ONE SIGN  
TRILLING ( $\pi^+$ )

NO. 2 N 510 DIETZGEN GRAPH PAPER  
SENSE UNIT WITH 50V  
SERIALS X-RAY VISION  
EUGENE DIETZGEN CO.  
MADE IN U.S.A.  
PER INTERACTING PROTON  
 $\frac{dN}{dp d\Omega}$

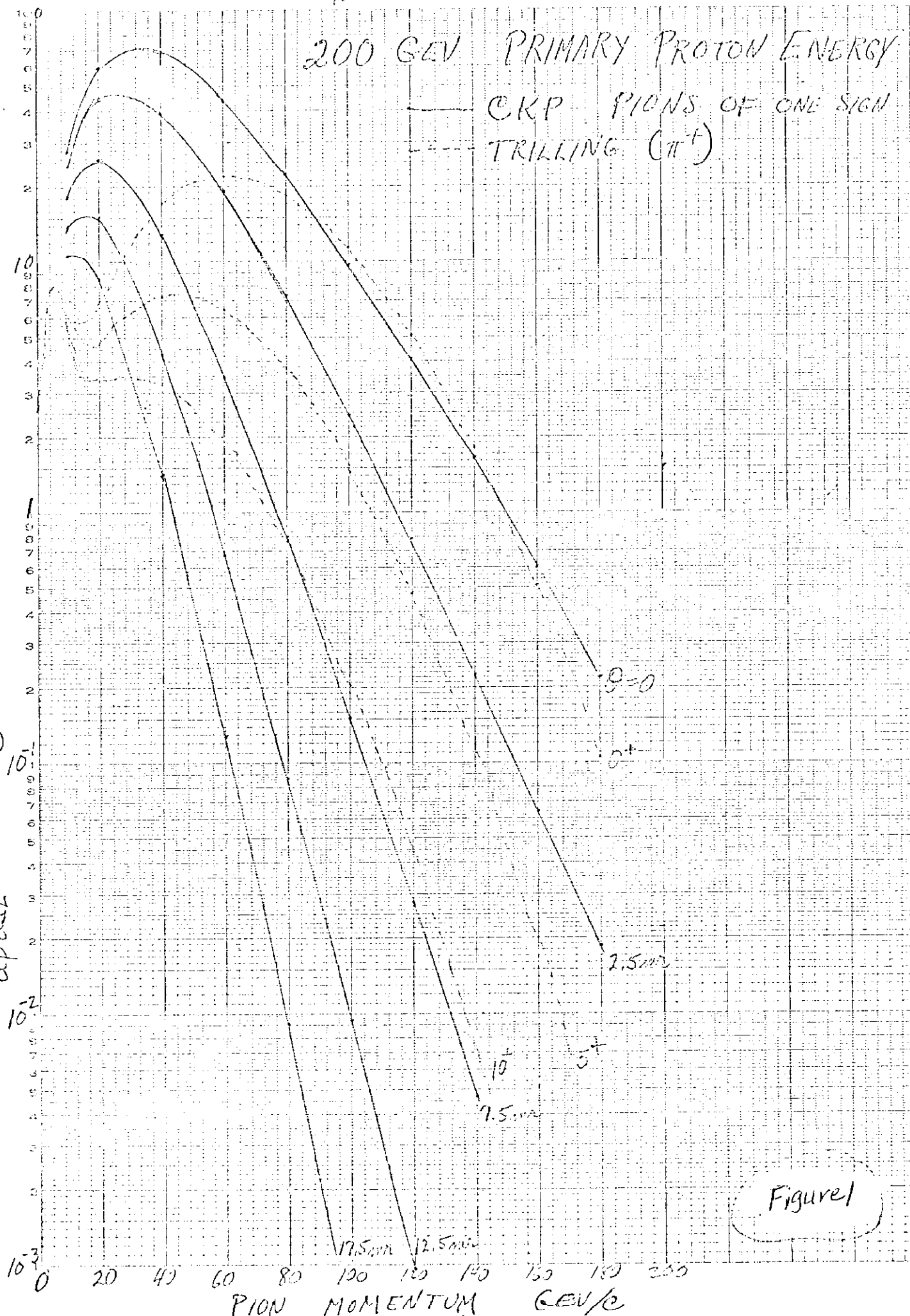


Figure 1

EUGENE DIETZEN SR.  
 MADE IN  
 INTERACTING PROTON  
 300 GeV  
 PER INTERACTING PROTON  
 10<sup>-3</sup>

300 GeV PRIMARY PROTON ENERGY  
 — CKP PIONS OF 1 CHARGE

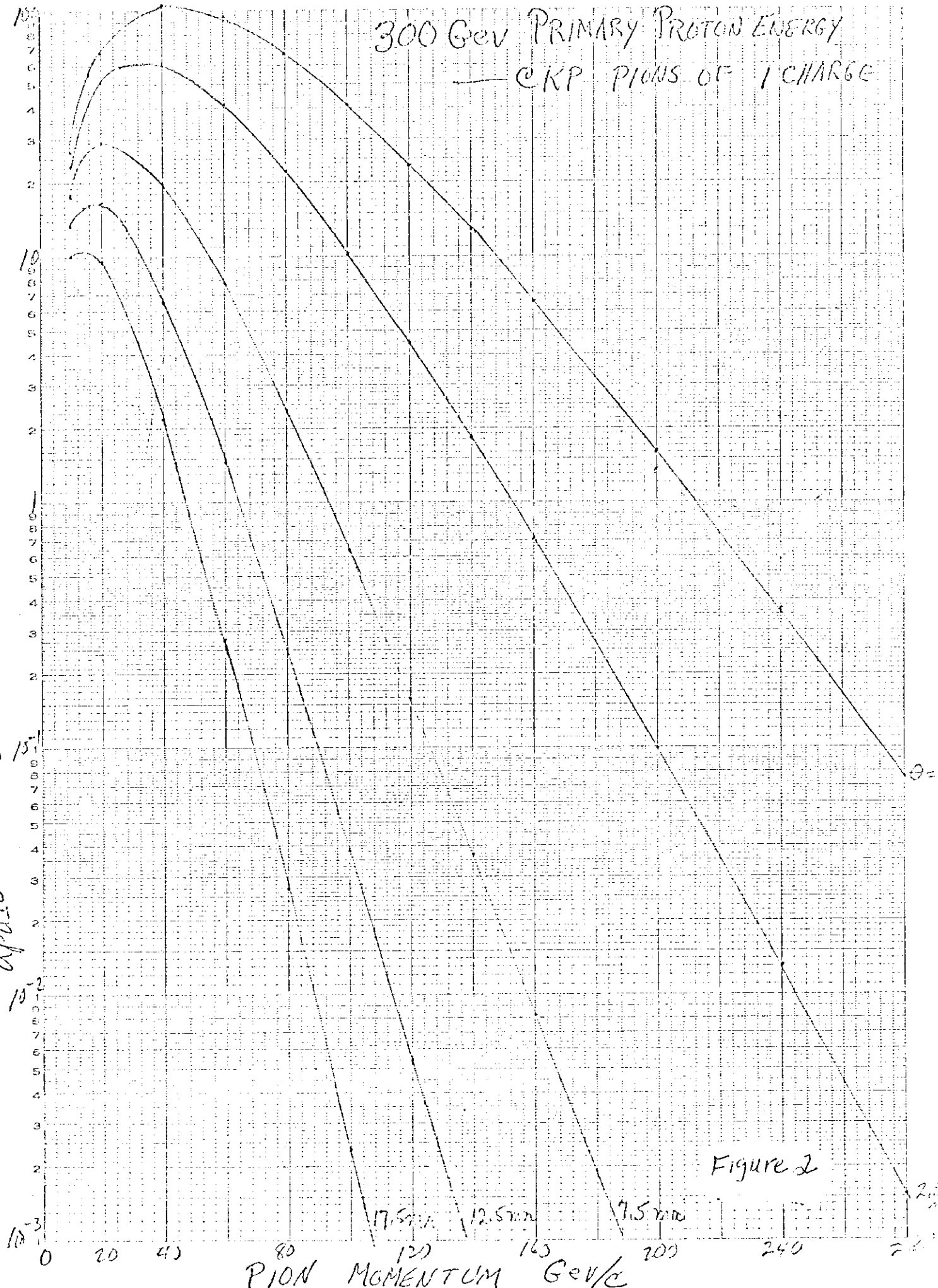


Figure 2

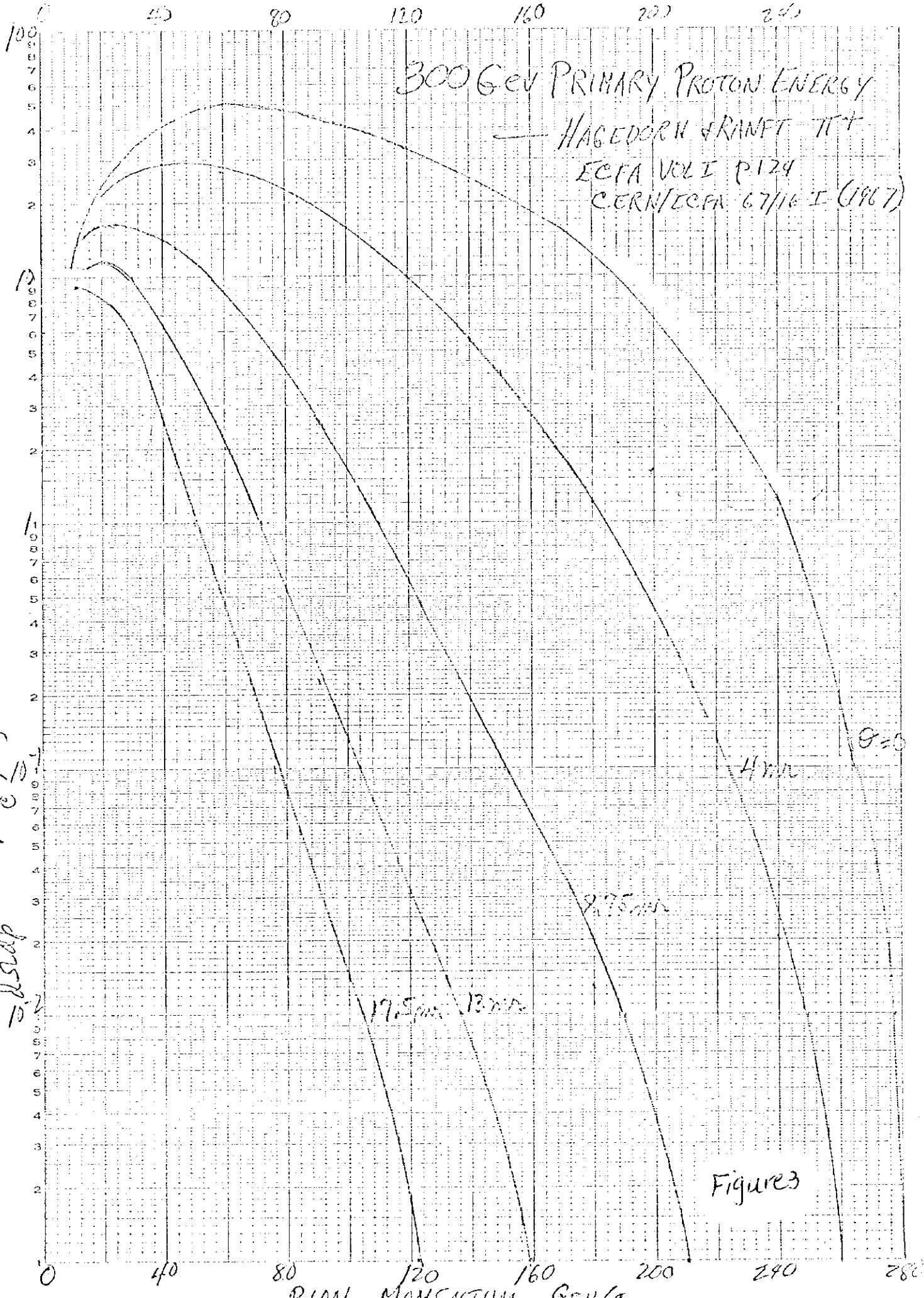
EUGENE DIETZGEN CO.  
MADE IN U. S. A.

NO. 40-LS10 DIETZGEN GRAPH PAPER  
SEMI-LOGarithmic

$\frac{dN}{dsdp} \frac{dN}{dV dE} / \text{GeV}^2 \text{SR}$ , INTERACTING PROTON

300 GeV PRIMARY PROTON ENERGY

HAGEDORN & RANFT  $\pi^+$   
ECFA VOL I P. 124  
CERN/ECFA 67/16 I (1967)



D<sub>3</sub>N-0-LSO DIETZGEN GRAPH PAPER  
 MADE IN U. S. A.  
 SUGENE DIETZGEN CO.

30 BEV PRIMARY PROTON ENERGY

CKP PIONS OF 1 CHARGE

ooo 1° ANDERSON ET AL

ooo 5.7° " " "

ooo 9.16° " " "

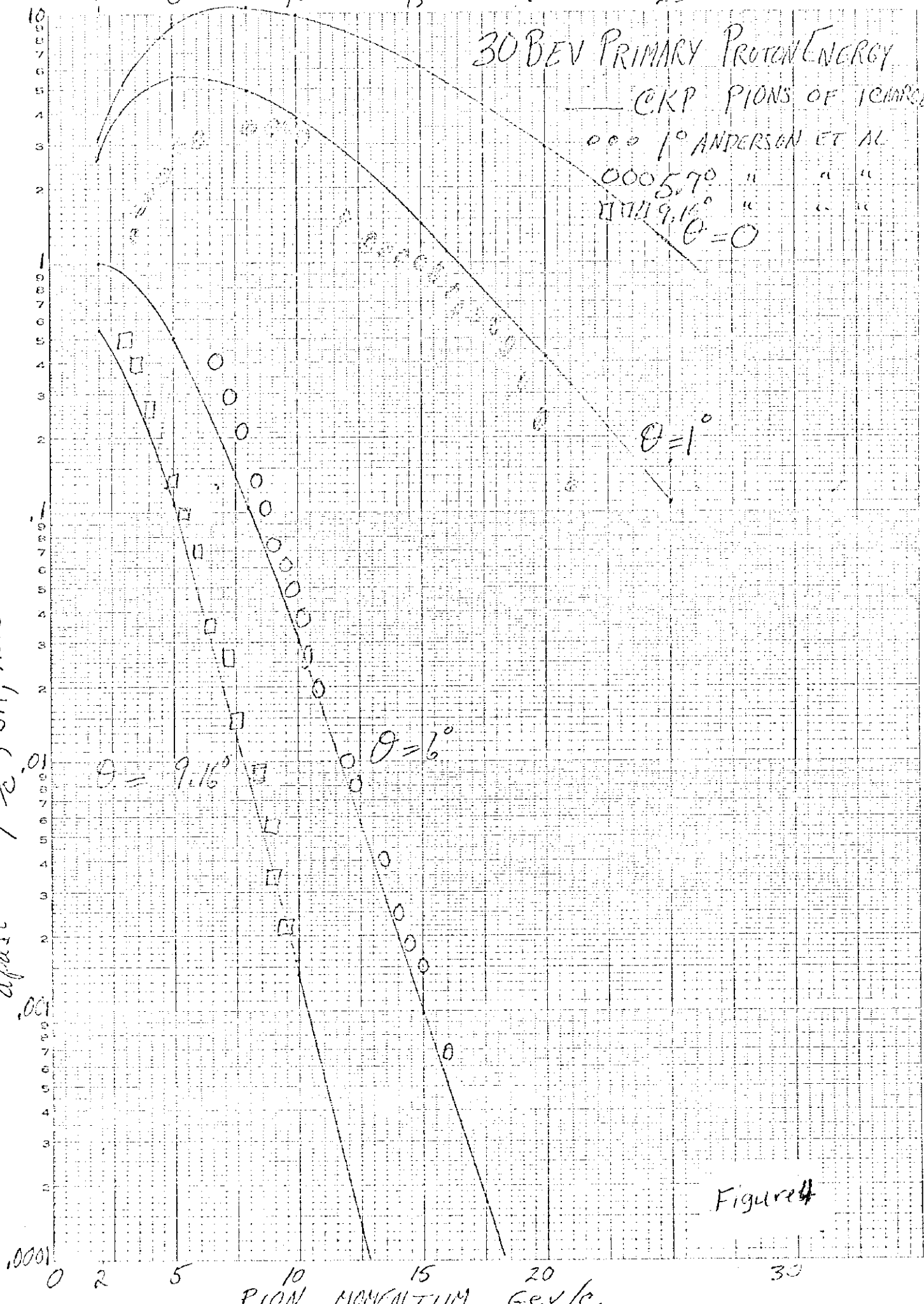
θ = 0

θ = 1°

θ = 6°

θ = 9.16°

Figure 4



NO. 3510 DIETZGEN CLAPH RADER  
 MADE IN PROTON  
 INTERACTING  
 PER  
 (C)

100 GeV PRIMARY PROTON ENERGY  
 — C.M.P. PIONS OF 1 CHARGE



Figure 5

EUGENE DIETZGEN CO.  
MADE IN U. S. A.

NEEDLE POINT METZGER GRAPH PAPER  
LOGARITHMIC

10<sup>2</sup> PER SR, INTERACTING PROTON, IN  $\pm \frac{1}{2}$  % MOMENTUM INTERVAL

100 GeV PRIMARY PROTON ENERGY

— C K P PIONS OF 1 CHARGE  
IN A  $\pm \frac{1}{2}$  % MOMENTUM INTERVAL



Figure 10

PION MOMENTUM, GeV/c

NO. 340-LS17 DIETZGEN 21/48 PAPER

10<sup>10</sup> p d p d s c  
5 10 p d p d s c  
EUGENE DIETZGEN CO  
MADE IN U.S.A.  
No. of Pions per ( $\pm 1.97$ ) Momentum Interval (SR)<sup>-1</sup>  
per Interacting Proton

20 40 60 80 100 120

200 GeV PRIMARY PROTON ENERGY  
CKP PIONS OF 1 CHARGE  
IN A ( $\pm \frac{1}{2}$ %) MOMENTUM INTERVAL

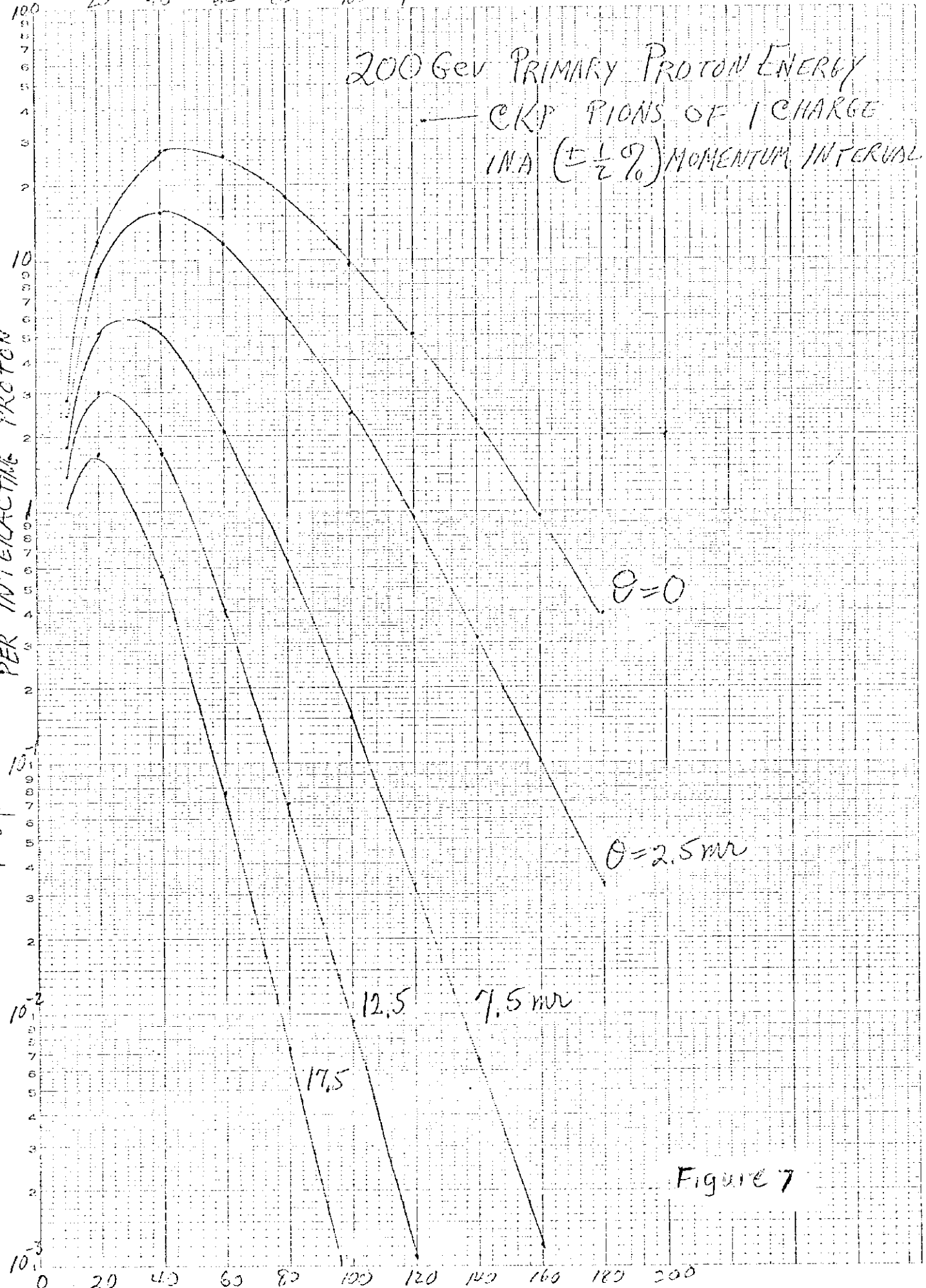
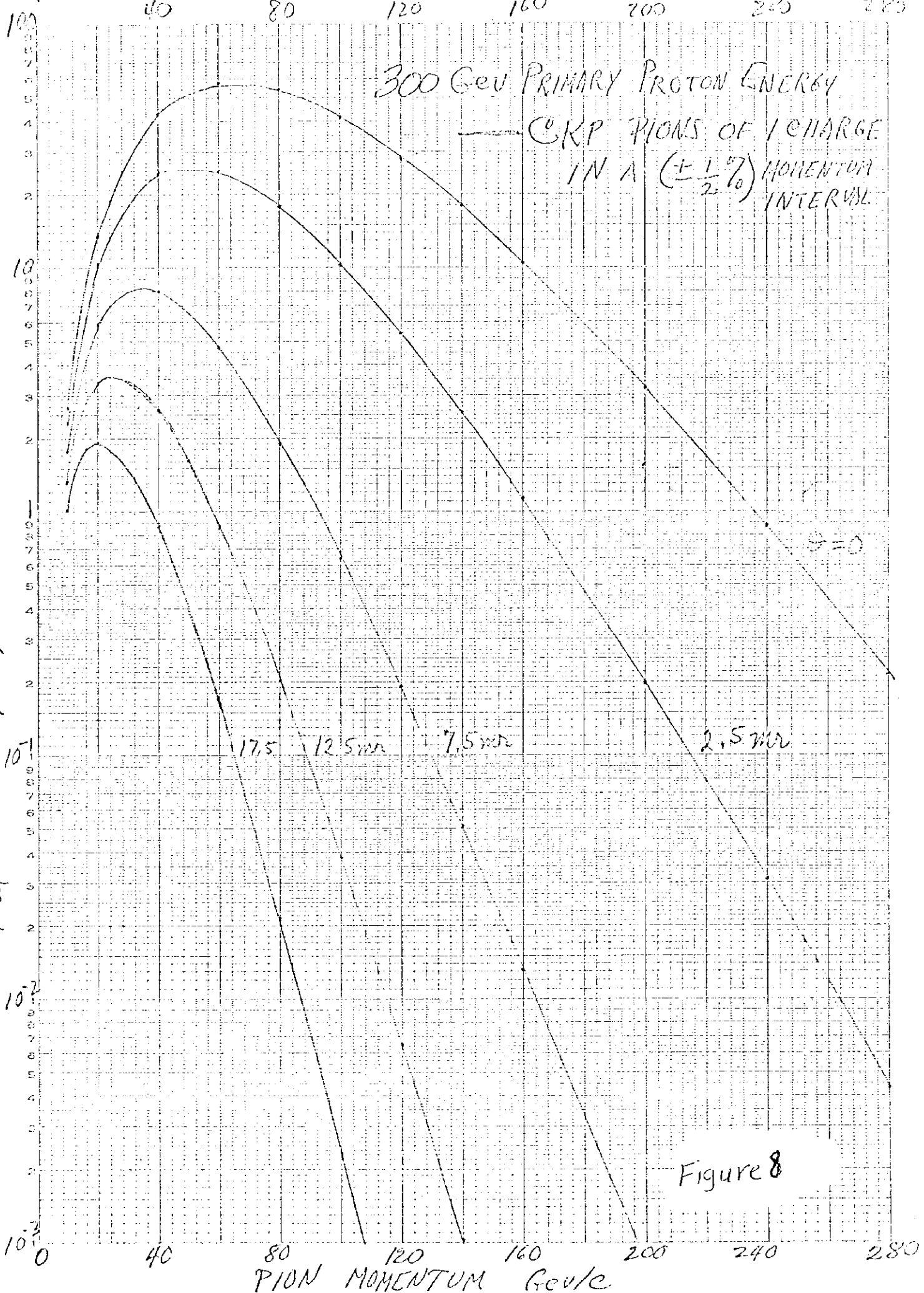


Figure 7

EUGENE DIETZEN CO.

NO. 340-147 METZEN GRAPH PAPER

10<sup>2</sup> PIONS PER SR, INTERACTING PROTON, IN  $\pm \frac{1}{2}\%$  MOMENTUM BIN



PION MOMENTUM GeV/c